# UV Resonance Raman Spectra and Molecular Orbital Calculations of Salicylic and Phthalic Acids Complexed to $Al^{3+}$ in Solution and on Mineral Surfaces

**Chad C. Trout and James D. Kubicki***

*Department of Geosciences and Materials Research Institute, The Pennsylvania State University, University Park, Pennsylvania 16802*

*Received: September 1, 2003; In Final Form: October 19, 2004*

Salicylic and phthalic acids have been used to study the complexation of aromatic carboxylic acids with Al(III) in solution and on mineral surfaces. A method for studying aqueous and surface carboxylic acids/metal complexes with UV Raman has been developed. The acids and Al(III) solutions were mixed in a 1:1 ratio at concentrations of 0.01 M. The mixtures were adjusted to pH 2.5 and 4 to be above and below the $pK_{a1}$ values of the carboxylic acids. The pH values of the acid solutions were based on the $pK_a$ values for the different acids to examine the neutral and charged species. The carboxylic acids were also adsorbed onto $Al_2O_3$. Comparisons between solution and adsorbed complexes were examined. Various possible types of complexes for the metal/acid complexes were modeled with ab initio molecular orbital/density functional theory calculations. The assignments of Al(III)-acid complexes were based on the best fits between experimental and model vibrational frequencies. Results are compared to previous speciation models based on potentiometric data.

## Introduction

At low concentrations, many metallic cations are necessary for important biological processes; but at high concentrations, they can be toxic.[1] Dissolved natural organic matter (NOM) is known to complex metallic cations in natural waters.[2] The chemistry of the NOM functional groups changes the solubility and bioavailability of dissolved metals and the dissolution rates of minerals. For example, acid rain precipitating onto soils is one important pathway where these reactions occur. As soils become saturated with low pH solutions during acid precipitation, metals present in the soil are flushed by the acidic porewater, thus increasing metal concentrations in the effluent.[3] As acid rain drains through the soil, metals, such as aluminum, interact with dissolved NOM. This results in the chemistry of the metal being influenced by organic functional groups and vice versa. The change in chemistry makes understanding the speciation of metallic ions in the environment important for determining environmental risk.

NOM is functionally defined,[4,5] and it is difficult to study analytically. As a result, model compounds known to have the same types of functional groups are often used as analogues for NOM.[6] Carboxylic acids, such as salicylic and phthalic acids, have been used to study the interaction of soluble organic acids and metal cations in the past[7,8] and were chosen here as a starting point for studies of the more complex natural materials such as fulvic and humic acids.

Despite much work on metal and organic acid complexes, spectroscopic studies to determine bonding mechanisms between simple organic acids and metal cations are commonly performed at concentrations higher than typically found in the environment. In addition, low pH values[7] are commonly used to prevent precipitation of Al-hydroxides. Hence, applying results from these types of spectroscopic studies to the environment can be difficult because speciation may change with concentration and pH.

Ideally, one would like to perform spectroscopic analyses on samples at similar concentrations and pH values as found in nature or on natural water samples themselves. However, this goal was not achievable with the current instrumentation available to us, but the UV resonance Raman technique has the capability to detect aqueous species down to $10^{-8}$ M. There are two advantages to working at lower concentrations: the results are more directly relevant to environmental concentrations and higher pH conditions can be used because Al is less likely to form precipitates. This work is an effort to bring the pH and concentration ranges accessible experimentally significantly closer (by at least 2 orders of magnitude) to the natural environmental conditions. Although further improvements in the technique are necessary, these results demonstrate the feasibility of collecting and modeling metal−organic complex vibrational spectra and point toward steps that could be taken to reach more environmentally relevant conditions. Results obtained under more realistic conditions may then be more directly applicable to environmental conditions.

Carboxylic acids in solution with $Al^{3+}$ and adsorbed to $Al_2O_3$ were studied with UV resonance Raman (UVRR) spectroscopy. There are three features of the ultraviolet excitation source for Raman spectroscopy that make the advances mentioned above possible. The first is that due to the charge acceleration inducing the emitted radiation, the scattering efficiency increases with the fourth power of the excitation frequency. The second advantage is that the excitation can occur within an absorption band for the molecule, hence the name UV resonance Raman. The third advantage is that fluorescence is not generally observed when NOM is excited in the UV region.

Experimental results were compared to calculated frequencies of the $Al^{3+}$−ligand complexes determined via ab initio, molecular orbital/density functional theory (MO/DFT) calculations on model species. Although spectroscopic methods provide information on molecular structure, interpretation of spectra is not always unambiguous. Ab initio calculations help interpret observed spectra because suggested models can be tested for their ability to reproduce observed vibrational frequencies and NMR chemical shifts.[9]

* Address correspondence to this author. E-mail: kubicki@geosc.psu.edu.

10.1021/jp036598p CCC: $27.50 
Published on Web 12/04/2004

There were two goals for this research. The first goal of this paper was to compare UVRR spectra of solution complexes and mineral surface complexes at various pH values. Aqueous-phase complexation of metal−carboxylate has been assumed to approximate the mineral surface−carboxylate complexes.[10] Hence, direct comparison of UVRR spectra from aqueous-phase and surface complexes can be used to test the validity of this assumption. The second goal was to model the observed vibrational frequencies of $Al^{3+}$−carboxylate complexes. Comparisons of the theoretical frequencies from various model complexes to the experimental results will indicate which model is most accurate.

## Experimental Section

**Solutions.** Salicylic and phthalic acids were obtained from Sigma Aldrich. Stock solutions of 0.1 M sodium perchlorate ($NaClO_4$) were made with 18 MΩ·cm ultrapure water from a Barnstead Nanopure. The carboxylic acids were added to the stock solutions to make $10^{-2}$ M solutions. The acid solutions were mixed in a 1:1 ratio with $10^{-2}$ M aluminum chloride solutions. The pH values selected were based on the p$K_a$ values of the different acids (to examine neutral and charge species) and the solubility of $Al^{3+}$. For example, the p$K_a$ values of salicylic acid are 2.8 and 13.8, so the solutions were set to pH 2.5 and 3.8 to produce dominantly the neutral and singly charged species, respectively. The p$K_a$ values of phthalic acid are 2.9 and 5.4, so the solution pH values were adjusted to 2.5, 4.0, and 7.0. The pH values were adjusted for several hours to ensure stability. Although a distribution of each species is likely to exist at a given pH, the deprotonation reactions of the acids were clearly visible in the spectra, so assigning peaks to a given species was straightforward.

**Adsorption.** The solid samples were prepared by placing 0.5 g of $Al_2O_3$ in a centrifuge tube with 25 mL of the carboxylic acid at a concentration of $10^{-2}$ M. The tubes were placed on a rototorque for about 17 h. The pH values of the solutions were adjusted during this time. The samples were then centrifuged and the supernatant decanted. Inner-sphere carboxylic acid surface complexes will generally be washed off only with basic solutions.[9] The $Al_2O_3$ was then washed with 18 MΩ ultrapure water from a Barnstead Nanopure to remove any outer-sphere or excess carboxylic acids. These samples were then centrifuged and the supernatant decanted. To minimize the presence of carboxylic acid in solution, the $Al_2O_3$ was placed on the inside face of the cuvette used for the UVRR spectra, and the excess liquid was allowed to flow to the bottom.

**Spectroscopy.** UVRR spectra were collected by using a signal-monochromatic configuration. A Coherent Innova 300 FReD intracavity frequency-doubled $Ar^+$ laser was used to produce the excitation wavelength of 257 nm. The sample was illuminated with a line focused by a cylindrical lens. This configuration interacts with a larger portion of the sample than spot illumination, which is helpful in reducing sample damage (i.e., photodegrading the organic ligand). The line illumination also provides for a better signal-to-noise ratio for the same input power as a spot configuration. The backscattered Raman signal was collected with a numerical aperture (0.5) reflecting objective. Two dielectric filters provided by Optical Omega were used to filter out the Rayleigh scattered light.[11] Approximately 30% of the Raman signal reached the UV sensitive liquid-nitrogen cooled CCD detector.

**Computational Methods.** Model vibrational frequencies were calculated with the Gaussian 98 program.[12] All calculations used hybrid MO/DFT with a Lee−Yang−Parr correlation functional,[13] a Becke 3-parameter exchange functional,[14] and 6-31G(d) basis sets.[15,16] The accuracy of this approach has been assessed in a previous paper on aqueous benzoic, salicylic, and phthalic acids.[17] Most model complexes were calculated in the gas phase. Explicit hydration of the complexes was necessary in a few cases to stabilize the protonation state of the complex. Calculated frequencies were scaled by 0.96.[18] The Gaussian checkpoint files were converted by using the freqcheck utility in the Gaussian program. The converted files were then used to animate vibrational motions of the molecules in Hyperchem 7.02 (Hypercube Inc. Gainesville, FL) to make assignments to the calculated and observed frequencies.

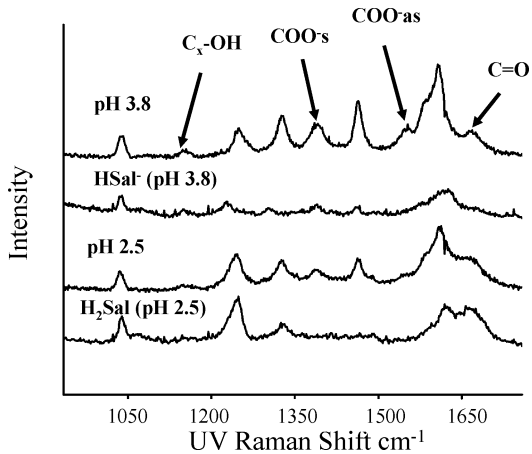


**Figure 1.** The UV resonance Raman spectra of salicylic acid at $10^{-2}$ M mixed in a 1:1 ratio with $10^{-2}$ M $AlCl_3$. The solution was studied at pH 2.5 and 3.8. The p$K_{a1}$ of salicylic is 2.8, thus both salicylic acid and salicylate were observed to complex to $Al^{3+}$. The peaks observed in salicylic acid are due to the ring structure, which are not effected by complexation according to the calculated models.

## Results/Discussion

**Salicylic and $Al^{3+}$ Solution.** The UVRR spectra of salicylic acid and $Al^{3+}$ solutions at pH 2.5 and 3.8 are shown in Figure 1. There were several differences between the two spectra. The first difference appears in the 1600-cm$^{-1}$ region (Figure 1). The peaks in this region became more defined as the pH was increased. The shoulders on either side of the main peak were better resolved at pH 3.8. The peak associated with the C═O stretch was observed at pH 3.8 (Table 1). The peaks associated with $COO^-$ symmetric (1386 cm$^{-1}$) and asymmetric (1548 cm$^{-1}$) stretches were observed at pH 2.5, but became more defined at the higher pH. The peak that appeared at 1489 cm$^{-1}$ at pH 2.5 was no longer observed at the higher pH, whereas the 1148-cm$^{-1}$ peak became more intense as the pH was increased.

Al−salicylate complex formation can be inferred by comparing the UVRR spectra of acid−metal solutions to the UVRR spectra of the acid alone in solution. The UVRR spectra of the carboxylic acids were previously reported and are shown in Figure 1.[17] While these solutions are mixtures of two protonation states of the compound, the minor species do not show up in the spectra nor do they interfere with identification of the peaks.[8,19,20] The observation of the $COO^-$ symmetric and asymmetric stretches in the Al−salicylate solution at pH 2.5 (Table 1) indicates complexation because salicylic acid alone at this pH is dominantly protonated and does not exhibit these modes in our previously measured spectra. The peaks observed in the salicylic only solution are due to the C−C ring stretches, which were not affected by the complexation.[8] Certain types of complexation do allow for the observation of the double bond.

The $COO^-$ symmetric peak for the Al−salicylate solution was comparable to its position for the UVRR spectra of

**TABLE 1: Experimental Peak Positions and Peak Assignments for Salicylic Acid and $AlCl_3$[a]**

| solution Sal/$Al^{3+}$ | | adsorbed Sal/$Al_2O_3$ | | | |
|---|---|---|---|---|---|
| pH 2.5 | pH 3.8 | pH 2.5 | pH 5 | pH 7 | peak assignments |
| 1661 | 1668 | | 1654 | 1659 | C═O |
| | | 1620 | 1616 | 1614 | C−C ring vibration |
| 1608 | 1607 | | | | C−C ring vibration |
| 1592 | 1587 | | | | C−C ring vibration |
| | | 1575 | 1573 | 1579 | C−C ring vibration |
| 1548 | 1548 | | | | $COO^-$ asymmetric |
| 1489 | | | | | C−C ring vibration |
| 1464 | 1464 | 1461 | 1465 | 1468 | C−C ring vibration |
| 1386 | 1391 | 1406 | 1392 | 1397 | $COO^-$ symmetric |
| 1327 | 1327 | 1326 | 1330 | 1348 | $C_x$CO-H/$COO^-$ symmetric |
| 1244 | 1249 | 1244 | 1249 | 1249 | $C_x$C−O |
| 1149 | 1149 | 1154 | 1157 | 1170 | C−H |
| | 1086 | | | | C−H |
| | | 1059 | 1064 | | C−H |
| 1038 | 1035 | 1035 | | | C−H |

[a] Experimental peak positions for salicylic and $AlCl_3$ in solution at $10^{-2}$ M at the two pH valuess studied are shown in the first two columns. The salicylic and $AlCl_3$ were mixed in a 1:1 ratio. The next three columns show the experimental peaks for salicylic absorbed to $Al_2O_3$ at various pH values. The assignments in the last column are based on the theoretical predictions and previous assignments, which are discussed in the text.

salicylate alone at pH 3.8 (Figure 1).[17] The asymmetric peak was shifted down from 1579 $cm^{-1}$ where it appeared for salicylate at pH 3.8. This downward shift of the $COO^-$ asymmetric was observed when the carboxylate group was complexed to $Al^{3+}$. The other peak of note was the C═O peak, which was not clearly observed for the salicylic acid solution. This was due to the deprotonation of the carboxylic group. The presense of a more defined C═O peak in the salicylic and $Al^{3+}$ solution indicated that the two C−O bonds in the carboxylic group were no longer identical, thus there was no resonance bonding as in salicylate.

Observation of a peak associated with the C═O stretch in the UVRR spectra indicated only one of the carboxylate oxygen atoms was bonded to $Al^{3+}$. The appearance of this stretch eliminates the possibility of the bridging bidentate complex (Figure 2D) through two carboxylate oxygen atoms. Biber and Stumm[6] observed a C═O stretch in an ATR-FTIR study of $Al^{3+}$−salicylate complexation in solution between pH 2 and 5. However, this peak occurred near 1720 $cm^{-1}$ in their ATR-FTIR study. A shoulder was present in the spectrum of Biber and Stumm[6] in a similar position to our observed C═O band between 1661 and 1668 $cm^{-1}$, but this peak was not well resolved from the H−O−H bending band of water centered around 1630 $cm^{-1}$.

The next peak of significance was the $C_x$−OH peak (1244 $cm^{-1}$). There was no significant shifting of the $C_x$−OH stretch in the UVRR spectrum. A shift of ∼10 $cm^{-1}$ upward for the Al−salicylate complex of the $C_x$−OH stretch has been observed by Biber and Stumm using ATR-FTIR.[6] This was attributed to a strengthening of the H-bond and not deprotonation.[8] When the phenol group deprotonates, the peak shifts by ca. +30 $cm^{-1}$.[8,20] Downward (negative) shifts of the peak indicate the phenol group was bonded to $Al^{3+}$.[8] This downward shift was observed for salicylic and $Fe^{3+}$ complexes.[8] This shift was not observed in our spectra for $Al^{3+}$−salicylate, so we conclude that the mononuclear bidentate structure does not form because this requires deprotonation of the phenol group (Figure 2C).

The $C_x$−OH stretch of the phenolic group in salicylic acid has been observed between 1245 and 1260 $cm^{-1}$.[6,8,20] At pH 14, Humbert et al. observed the $C_x$−$O^-$ peak in the phenolic group of salicylate at 1265 $cm^{-1}$ which was ca. +20 $cm^{-1}$ shifted from the neutral species of salicylic acid in their spectra.[20] In the Humbert et al. study on phenol, the $C_x$−$O^-$ peak was observed to increase ca. +30 $cm^{-1}$ from the C−OH peak.[21] Hence, we expect a similar shift if deprotonation of the phenolic group in salicylic acid should occur. For an accurate comparison, a solution of salicylate run on the same instrument was essential for stating whether the phenolic group was deprotonated or not. Because we did not observe a significant frequency increase for this mode between the pH 2.5 and 3.8 spectra, the experimental data suggest that the monodentate structure (Figure 2A,B) was the most likely possibility for both pH 2.5 and 3.8. This was in agreement with Biber and Stumm [6] and Kubicki et al.,[9] but not with Thomas et al.,[7] who concluded that salicylic acid and $Al^{3+}$ would form the mononuclear bidentate structure at pH 3.3 based on NMR spectra and potentiometric speciation diagrams.

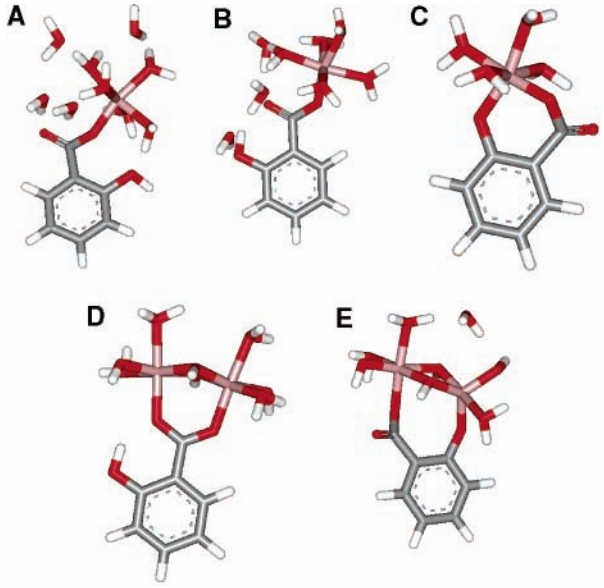


**Figure 2.** The optimized structures for the different complexes of salicylate and $Al^{3+}$ are shown. The structures are (A) monodentate with an H-bond to the oxygen bonded to $Al^{3+}$, (B) monodentate with the H-bond to the oxygen doubly bonded to carbon, (C) mononuclear bidentate, (D) bridging bidentate through the carboxylic group, and (E) bridging bidentate through the phenol and carboxylic group.

The structures chosen for optimization were two mononuclear monodentate structures (Figure 2A,B), a mononuclear bidentate complex (Figure 2C), and two bridging bidentate structures (Figure 2D,E) because these complexes have been suggested in the past.

The mononuclear bidentate (Figure 2C)[7,22,23] and mononuclear monodentate (Figure 2A) structures[6,9] were chosen because they have been predicted to represent the complexes of $Al^{3+}$ and/or $Al_2O_3$ with salicylic acid. Two different monodentate structures were optimized. In the first (Figure 2A), the intramolecular H-bond from the phenolic group was initially to the oxygen bonded to $Al^{3+}$; however, the energy-minimized structure resulted in the phenol group rotating away from the Al−O−C oxygen atom. In the second configuration (Figure 2B), the H-bond from the phenolic group was to the C═O oxygen. Previously, the H-bond had been shown to the Al−O−C oxygen atom.[6,9] The stronger H-bond should result from the interaction of the C═O oxygen, because it would have the higher electronegative charge.

The bridging bidentate structure linked via the two carboxylate O atoms (Figure 2D) was optimized and evaluated because it was predicted for the salicylic/$Fe^{3+}$ complex[8] and other

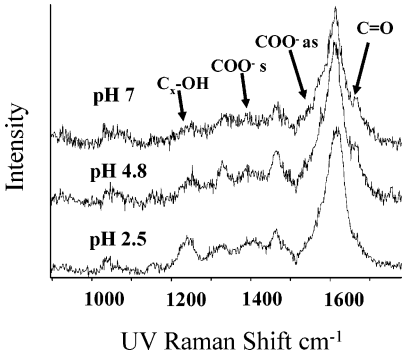


**Figure 3.** UVRR spectra of salicylic acid adsorbed to $Al_2O_3$ at pH values of 2.5, 4.8, and 7. These correspond to the neutral and anionic species of salicylic acid. The bianionic species was not studied, due to the strong basic solutions needed, which would react with the quartz cuvette.

carboxylic and $Al^{3+}$ complexes.[7,22−24] The second bidentate configuration with one oxygen atom from the carboxylate group and one from the phenolate group bonded to an Al atom was tested for comparison. Other authors have suggested a mononuclear bidentate mechanism (Figure 2C) for salicylate complexation to $Al^{3+}$ with the phenolate participating in bonding to $Al^{3+}$.[7,25] Comparisons of the frequencies calculated from these complexes with the observed frequencies will be discussed below (see the Theoretical Calculations section)

**Salicylic Acid Adsorbed onto $Al_2O_3$.** The UVRR spectra for salicylic acid adsorbed onto $Al_2O_3$ at pH values of 2.5, 5, and 7 are shown in Figure 3. As the pH was increased, the signal-to-noise ratio decreased. One feature that stood out in the UVRR spectrum at pH 2.5 was the absence of the C═O peak observed between 1660 and 1670 $cm^{-1}$ in the aqueous solution spectra. This indicates that the monodentate structure (Figure 2A,B) cannot be the surface complex. If the structure were mononuclear bidentate or bridging bidentate through the phenol group (Figure 2C,E), then the peak associated with the $C_xC-O$ stretch (1244 $cm^{-1}$) should be shifted down from its position in salicylate (1244 $cm^{-1}$). Because no shift was observed, these two structures were ruled out as possibilities for the surface complex. The other peak of importance for determining the structure of the complex was the $COO^-$ symmetric peak. The peak was shifted from 1390 $cm^{-1}$, where it was observed for salicylate,[17] to 1406 $cm^{-1}$ for the adsorbed sample (Table 1). A shift upward of this peak has been interpreted previously as a bridging bidentate structure for acetate with an aqueous $Ga_2(OH)_2(OH_2)_6$ dimer.[26] The bridging bidentate structure appears to be the most likely possibility based on these results.

For the samples adsorbed at pH 4.8 and 7, the C═O stretch is present between 1654 and 1659 $cm^{-1}$. This indicates that the bridging bidentate structure (Figure 2D) does not represent the structure of the surface complex under these pH conditions. As in the sample at pH 2.5, the $COO^-_{as}$ was not clearly resolved within the broad band centered near 1600 $cm^{-1}$, which is due to phenyl ring vibrational modes.[8] At pH 4.8, the $COO^-$ symmetric stretch appears at 1392 $cm^{-1}$, which is comparable to aqueous salicylate.

The $C_x-OH$ mode was slightly shifted to 1249 $cm^{-1}$ from its position of 1245 $cm^{-1}$. This small change is associated with changes in H-bonding to the phenol group rather than deprotonation;[8] hence, the bidentate configurations involving deprotonation of the phenol group (Figure 2C,E) are unlikely. For the sample at pH 7, similar results to the sample at pH 4.8 were observed. We conclude that the structure of the surface complexes at pH 4.8 and 7 is the monodentate configuration (Figure 2B).

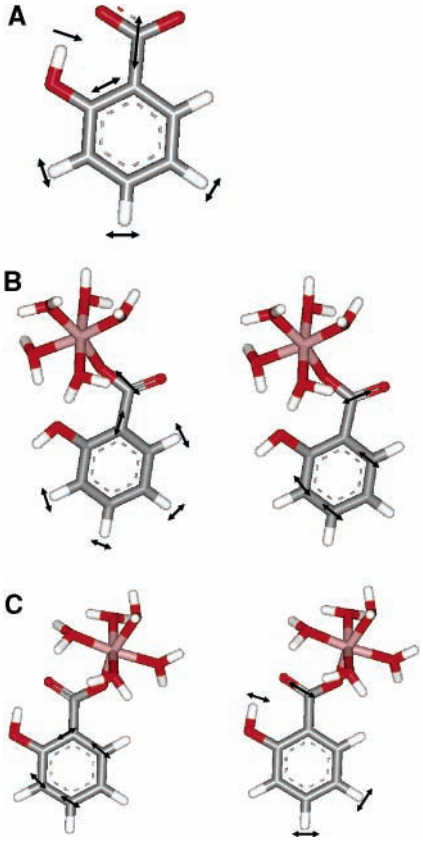


**Figure 4.** The vibrational modes of the $COO^-$ asymmetric and symmetric stretches compared between the modeled salicylate and $Al^{3+}$/salicylate complex: (A) salicylate $COO^-$ symmetric mode; (B) the monodentate model with no H-bond between the phenol and carboxylic group; and (C) the monodentate model with a H-bond between the phenol and carboxylate group.

**Theoretical Calculations.** The two-monodentate structures were optimized to determine the effect of phenolic H-bonding on the structure and vibrational frequencies. As observed in Figure 2A, a H-bond from the phenolic group to the oxygen bonded to $Al^{3+}$ did not exist in this configuration. The calculation was restarted numerous times in the attempt to keep the H-bond in place, but the resulting lack of a H-bond was always the same. In contrast, Figure 2B optimized to produce the H-bond to the double-bonded oxygen atom. The positions of the $COO^-$ symmetric stretch and the C═O stretch were similar for both structures (Figure 2A: $COO^-_s$ = 1350 $cm^{-1}$ and C═O = 1637 $cm^{-1}$; Figure 2B: $COO^-_s$ = 1347 $cm^{-1}$ and C═O = 1626 $cm^{-1}$). There was more difference in the $COO^-$ asymmetric stretch with Figure 2A at 1595 $cm^{-1}$ and Figure 2B at 1531 $cm^{-1}$. Even though many of the peaks were in close agreement, the correlation with observed frequencies based on Figure 2B had fit the data better than frequencies calculated with the structure in Figure 2A.

In the discussion above, the $COO^-$ symmetric and asymmetric stretches as well as a C═O stretching modes were mentioned as being present in the monodentate Al−salicylate complex. This conclusion is based on an analysis of the vibrational modes as output in Gaussian 98, using the visualization software HyperChem 7.02 (Hypercube Inc. Gainesville, FL). Figure 4 illustrates the components of each of these modes to clarify what is meant by the terminology employed here. This distinction is made here because previous literature has assigned bands to either C−O and C═O (when the COOH group is present) or $COO^-_s$ and $COO^-_{as}$ (when the $COO^-$ group is present). Here,

**TABLE 2: Calculated $\delta^{27}$Al Values for the Optimized Models Shown in Figure 2[a]**

| molecule | $\sigma Al^{3+}$ | $\delta Al^{3+}_{(theory)}$ | $\delta Al^{3+}_{(expt)}$ |
|---|---|---|---|
| $[(HSal^{-})Al^{3+}(H_2O)_5]\cdot 4H_2O$ | 627 | 6 | 3 |
| $[(HSal^{-})Al^{3+}(H_2O)_5]\cdot 4H_2O$ (2b) | 626 | 7 | |
| $[(Sal^{-2})Al^{3+}(H_2O)_4]$ | 616 | 17 | |
| $[(HSal^{-})Al_2(OH)_4{}^{+4}(H_2O)_4]$ | 636 | -3 | |

[a] The experimental data are taken from Thomas et al., ref 7.

we show in comparison to salicylic acid that there are three modes present when the carboxylate group is bonded to $Al^{3+}$.

The asymmetric and C═O cannot be differentiated for the monodentate structures (Figure 4) based solely on the carboxylate group stretches. The stretches are very similar. The difference was in the benzene ring stretches, which are coupled to the asymmetric and C═O stretches. The $COO^{-}$ symmetric stretch does not appear as a true symmetric stretch. This vibrational mode is similar in character to the asymmetric stretch at higher frequency (Figure 4). While all three peaks normally associated with these modes were observed, the actual vibration modes were not the same as past assignments of these modes. These differences in the stretches from the previous observations of the acids in solution can be attributed to the Al−O bond.

At pH 2.5 for the solution of salicylic and $AlCl_3$, the bridging bidentate structure, $[(HSal)Al_2(OH)_2(H_2O)_6]^{3+}$ (Figure 2D), had the best correlation with a slope of 1.00, standard deviation of 12.59, and an $R^2$ of 1.00 (Table 3). This was not in agreement with the UVRR data which suggested a monodentate structure (Table 4), nor with Biber and Stumm,[6] who also suggested a monodentate structure (Figure 2B) at this pH based on the presence of a C═O stretch. The fit for the monodentate structure was almost as accurate with a slope of 1.00, standard deviation of 14.39, and an $R^2$ of 1.00. The distinguishing feature of the observed spectrum is the C═O peak at 1661 $cm^{-1}$. The monodentate structure has a calculated C═O stretch at 1626 $cm^{-1}$, and the bidentate bridging complex has a C−C ring mode at 1618 $cm^{-1}$. Consequently, we cannot distinguish definitively based on the model calculations which of these complexes gave rise to the observed frequencies from these calculations. The B3LYP/6-31G(d) method may not be accurately reproducing the frequency of C═O modes due to the importance of electron correlation in these types of bonds.[27] The best evidence we have for assigning the Al−salicylate complex at pH 2.5 to the monodentate structure is the presence of the C═O peak and the agreement between the calculated and observed $^{27}$Al NMR chemical shifts[7] (Table 2). The calculated NMR chemical shift for the bridging bidentate structure in this study is −3 ppm.

The bridging bidentate (Figure 2D) structure also gave the best correlation for the adsorbed sample at pH 2.5 with a slope of 1.01, standard deviation of 8.74, and an $R^2$ of 1.00 (Table 3). This result was in agreement with the UVRR data (Table 4), which suggested a bridging bidentate structure (Figrue 1d). This structure was previously suggested for salicylate complexes forming on illite clay at low pH.[9]

For solutions and adsorbed samples at higher pH, the monodentate structure was predicted with the UVRR data. The correlation with the monodentate structure also gave the best fit for all the samples, which was in agreement with interpretations of Biber and Stumm and Kubicki et al.[6,9] The structure of mononuclear bidentate (Figure 2C) predicted by Thomas et al.[7] was not supported by the UVRR experimental data nor by the theoretical calculations.

**Calculated $^{27}$Al NMR Chemical Shifts for $Al^{3+}$−Salicylate Complexes.** Thomas et al.[7] performed NMR experiments on solutions of $Al^{3+}$ and salicylic acid. NMR calculations were performed on the optimized structures to determine whether the monodentate, mononuclear bidentate, or the bridging bidentate could reproduce the observed $^{27}$Al NMR chemical shift ($\delta^{27}$-Al). A broad shoulder at 3 ppm has been reported for $^{27}$Al NMR spectra of $Al^{3+}$−salicylate complex at pH 3.3.[7] The mononuclear bidentate $[(Sal^{2-})Al^{3+}(H_2O)_4]$ structure was assigned to this NMR result by Thomas et al. (Figure 1c).[7] Kubicki et al. performed optimizations with the Hartree−Fock 3-21G(d,p) basis set and NMR calculations with Hartree−Fock 6-31G(d) on some of the structures in Figure 1 to calculate $\delta^{27}$Al values.[28] Those calculated results predicted that the monodentate structures (Figure 2A,B) would have a shift of 6 whereas the mononuclear bidentate and bridging bidentate complexes would have $\delta^{27}$Al shifts of ca. 16 and 8 ppm, respectively.

Optimizing the structures at the B3LYP/6-31G(d) level and NMR calculations at the HF/6-31G(d) level produced $\delta^{27}$Al calculated shifts of 6 and 7 ppm for the monodentate structures (Figure 2, A and B, respectively) and 17 ppm for the mononuclear bidentate structure (Table 2). These results were in agreement with the structures optimized at the HF/3-21G(d,p) level. The bridging bidentate structure optimized with B3LYP/6-31G(d) had a calculated $\delta^{27}$Al value of −3 ppm, which differed significantly from the $\delta^{27}$Al shift of +8 ppm of the

**TABLE 3: Linear Fit Parameters from the Correlations of Experimental Data vs Theoretical Data for the Solutions of Salicylic and Aluminum at 0.01 M and Salicylic Adsorbed to $Al_2O_3$[a]**

| | | Figure 2B | | | Figure 2A | | | Figure 2C | | | Figure 2D | | | Figure 2E | | |
|---|---|---|---|---|---|---|---|---|---|---|---|---|---|---|---|---|
| sample | pH | slope | SD | $R^2$ | slope | SD | $R^2$ | slope | SD | $R^2$ | slope | SD | $R^2$ | slope | SD | $R^2$ |
| Sal−$AlCl_3$ | 2.5 | 1.00 | 14.39 | 1.00 | 1.02 | 12.16 | 1.00 | 1.05 | 31.26 | 0.98 | 1.00 | 12.59 | 1.00 | 1.03 | 17.32 | 0.99 |
| | 3.8 | 1.00 | 12.52 | 1.00 | 1.01 | 16.04 | 1.00 | 1.04 | 22.43 | 0.99 | 1.00 | 13.37 | 1.00 | 1.03 | 16.18 | 1.00 |
| Sal−$Al_2O_3$ | 2.5 | 1.04 | 17.22 | 0.99 | 1.03 | 18.30 | 0.99 | 1.05 | 22.74 | 0.99 | 1.01 | 8.74 | 1.00 | 1.03 | 17.83 | 0.99 |
| | 5 | 1.00 | 14.67 | 0.99 | 0.95 | 23.07 | 0.99 | 1.00 | 31.36 | 0.98 | 0.97 | 12.35 | 1.00 | 1.00 | 23.37 | 0.99 |
| | 7 | 1.01 | 10.36 | 1.00 | 0.99 | 21.99 | 0.99 | 1.03 | 31.77 | 0.98 | 0.97 | 15.41 | 0.99 | 1.02 | 21.80 | 0.99 |

[a] The figures for the optimized structures are shown in Figure 2, which corresponds to the listing for the columns.

**TABLE 4: Summary of the Predicted Structures for the Different Methods Used To Study the Samples**

| sample | pH | UVRR | NMR[a] | theoretical[b] |
|---|---|---|---|---|
| Sal−$AlCl_3$ | 2.5 | monodentate | monodentate | bridging bidentate |
| | 3.8 | monodentate | | monodentate |
| Sal−$Al_2O_3$ | 2.5 | bridging bidentate | | bridging bidentate |
| | 5 | monodentate | | monodentate |
| | 7 | monodentate | | monodentate |

[a] Theoretical calculations compared to previous results from Thomas et al., ref 7. [b] The theoretical frequencies calculated were compared to UVRR.

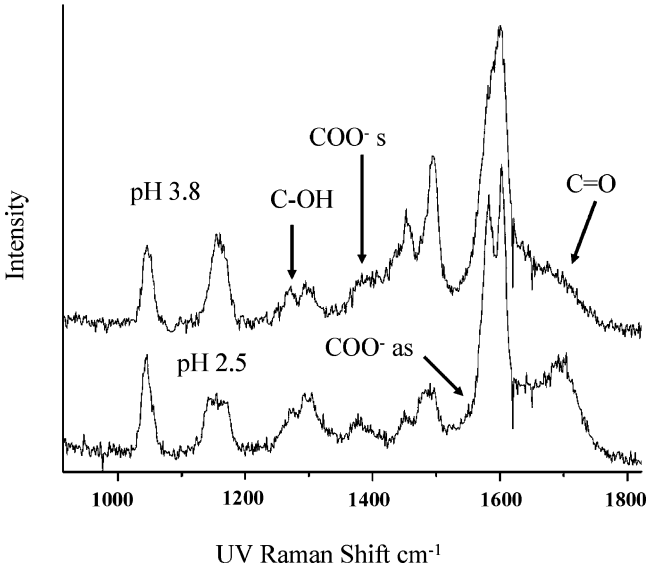


**Figure 5.** UVRR spectra of phthalic acid at $10^{-2}$ M mixed in a 1:1 ratio with $10^{-2}$ M $AlCl_3$. The solution was studied at pH 2.5 and 3.8. The $pK_{a1}$ of salicylic was 2.9, thus phthalic and phthalate were observed to complex to $Al^{3+}$.

structure optimized at the HF/3-21G(d,p) level.[28] Regardless of the method used, comparison of the theoretical NMR results and the experimental results of Thomas et al. [7] show that the monodentate configuration is most consistent with both the NMR and UVRR spectra.

**Phthalic Acid.** *Phthalic Acid and $Al^{3+}$ Solution.* The UVRR spectra of phthalic acid and $Al^{3+}$ at pH 2.5 and 3.8 are shown in Figure 5. The UVRR spectra of phthalic acid only in solution at pH 2.5 showed a doublet for the C═O peak.[17] This feature was not observed at pH 2.5 for phthalic/$Al^{3+}$ solution possibly indicating a type of bridging bidentate structure according to the arguments above (Figure 6A−D). Two peaks associated with the $COO^-$ symmetric stretch appeared at 1378 and 1405 $cm^{-1}$ for the solution of phthalic/$Al^{3+}$. The $COO^-$ symmetric stretch was observed at 1375 $cm^{-1}$ for phthalate in solution.[17] The $COO^-$ asymmetric peak was not observed in the UVRR spectra for this solution.

If the structure is where one $Al^{3+}$ was in a bridging bidentate through one oxygen atom of each group or a mononuclear monodentate structure (Figure 6, C, D, F), then one would expect to observe a doublet for the C═O stretch. The doublet has been observed for UVRR,[17] Raman experiments on solid single crystals of phthalic acid,[29] and surface enhanced Raman scattering with phthalic and silver in solution.[19] Experiments performed with FT-IR in solution failed to observe the C═O doublet.[30] From these results, we would expect that it would be possible to observe the C═O doublet if the structures in C, D, or F of Figure 6 were the correct structures, thus ruling them out as possibilities for the complex of phthalic/$Al^{3+}$. Normally, an upward shift of the $COO^-_s$ peak, for carboxylic acids, other than salicylic due to the strong intramolecular H-bond, indicates a bridging bidentate structure of some type. A downward shift would indicate a monodentate complex. The peak observed at 1378 $cm^{-1}$ could be due to excess phthalic acid in the solution and not attributed to the bridging bidentate through two carboxylic groups, because it is close to the 1375-$cm^{-1}$ peak observed with phthalate in solution.

At pH 3.8, the C═O stretch was observed as a broad peak. The peaks that appear at 1579 and 1599 $cm^{-1}$ for the solution at pH 2.5 have broadened into one peak at 1599 $cm^{-1}$ pH 3.8. The peaks attributed to C−C stretching in the 1400−1500 $cm^{-1}$ range become more intense with the increase in pH. The peak at 1426 $cm^{-1}$ could be attributed to either a C−C ring vibration or the $COO^-$ symmetric peak shift, which would be consistent with previous reports of this mode shifting with complexation to other metals.[31] Peaks attributed to the $COO^-$ symmetric stretch also appear at 1383 and 1353 $cm^{-1}$. The first peak was shifted by +9 $cm^{-1}$ from the peak position of phthalate in solution, whereas the second was shifted by −33 $cm^{-1}$.[17]

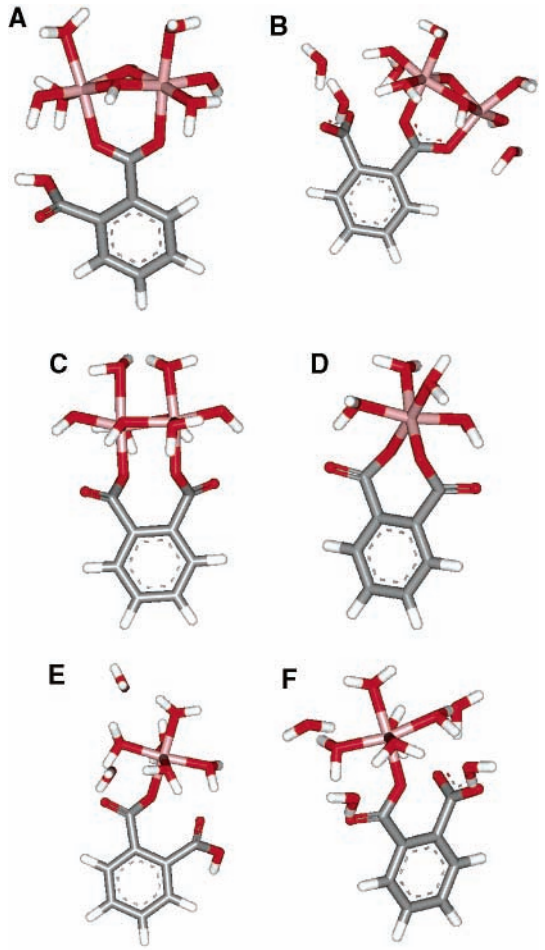


**Figure 6.** The optimized structures for the different complexes of phthalate and $Al^{3+}$ are shown. The structures are (A) bridging bidentate, (B) deprotonated bridging bidentate, (C) bridging bidentate through two carboxylic groups, (D) mononuclear bidentate, (E) monodentate, and (F) deprotonated monodentate.

The broadening of the peaks at pH 3.8 and the observance of three peaks possibly attributed to the $COO^-$ symmetric stretch possibly indicate more than one type of complex was being formed. The observance of the symmetric stretch at 1426 $cm^{-1}$, if attributed to the $COO^-$ asymmetric stretch, indicates a bridging bidentate structure through one carboxylate group. The peak observed at 1383 $cm^{-1}$ was in the same region the $COO^-$ peak for a bridging bidentate structure through one oxygen of two carboxylic groups has been predicted for adsorbed species,[22] but it could be due to excess phthalic acid. The 1353-$cm^{-1}$ peak indicates a monodentate structure, which was in agreement with the observed position for the complex of phtahlate adsorbed to Fe.[31]

The optimized structures for phthalic acid and $Al^{3+}$ complex are shown in Figure 6. These structures have been previously predicted for either $Al^{3+}$−phthalate complexes or other metal−carboxylate complexes. The bridging between one oxygen of each carboxylic group to an individual $Al^{3+}$ ion was predicted as the structure for the complex between phthalate and several

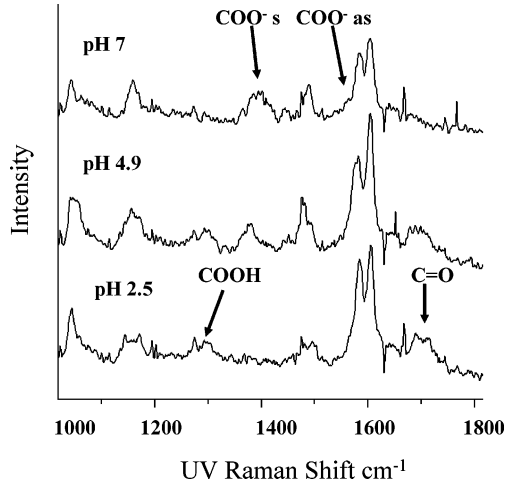


**Figure 7.** UVRR spectra of phthalate adsorbed to $Al_2O_3$ at pH values of 2.5, 4.9, and 7. These pH values correspond to predominantly the neutral, anion, and bianion forms of phthalic acid.

metals (Figure 6c).[22] For phthalate and goethite (α-FeOOH, an Fe counterpart that has a similar surface structure to the hydrated $Al_2O_3$ used in this study) the two structures that have been assigned are a bridging bidentate structure through two oxygen atoms in one carboxylic group (Figure 6, A or B) and the monodentate structure (Figure 6, E or F).[31] The rest of the structures were predicted in various metal−carboxylate complexes,[7,9] and thus were modeled as alternatives to the previously predicted structures.

*Phthalic Acid Adsorbed onto $Al_2O_3$.* The UVRR spectra for phthalic acid adsorbed to $Al_2O_3$ at pH values of 2.5, 5, and 7 are shown in Figure 7. At pH 2.5 the peak attributed to the C═O stretch was observed, but it was not well defined. The C═O peak was not observed at the higher pH values, but the 1600-$cm^{-1}$ peak had a small shoulder that may indicate the presence of C═O (Figure 7). The peak centered at 1600 $cm^{-1}$ was broad and hinders the observation of the peaks in the 1500−1600 $cm^{-1}$ region, so the $COO^-_{as}$ was not observed at pH 2.5 and 5. $COO^-_{as}$ was observed at pH 7, which was not shifted from the position for phthalate (Table 5). The $COO^-$ symmetric stretch was observed in the 1400−1415 $cm^{-1}$ region for the adsorbed samples, which was shifted from 1375 $cm^{-1}$ for phthalate (Table 5). There was also a second peak attributed to the carboxylate symmetric stretch for pH 5 and 7 at 1341 and 1364 $cm^{-1}$, respectively (Table 5). For the sample at pH 2.5, it would appear that a bridging bidentate structure through one carboxylic group would be the structure of the complex due to the similarity with the solution results (Figure 6A).

For the samples at pH 5 and 7 there were two types of complexes. The shift to above 1400 $cm^{-1}$ for the $COO^-$ symmetric peak and the observation of the C═O peak indicates a bridging structure complex was formed.[31] Which type (Figure 6, B or C) of bridging structure could not be identified from experimental evidence due to the broadening of the peaks from multiple complexes. The presence of a monodentate structure was indicated by the shift of the carboxylate symmetric peak to 1341 $cm^{-1}$ for pH 5 (Figure 6A). In the sample at pH 7, the second $COO^-$ symmetric peak was observed at 1362 $cm^{-1}$ (Table 5), which may be too high for a monodentate structure compared to previous reports.[31] This could possibly indicate that one of the bridging bidentate structures (Figure 6, A−D) was representative of the complex.

**Theoretical Calculations.** A comparison of $\Delta\nu$ ($\Delta\nu = \nu_{as} - \nu_s$) between the ion in solution and the metal complex could give an indication of the type of complex being formed.[8,31] These comparisons were based on single-crystal studies of metal carboxylates.[32] If the value of $\Delta\nu$ were larger for the ion in solution, then a bridging bidentate complex would be predicted. This would be supported by a shift up of the $COO^-$ symmetric stretch. If the complex had the larger value, then a monodentate structure would be the predicted structure, which is indicated by a downward shift of the $COO^-$ symmetric peak. The calculated positions for the $COO^-$ symmetric and asymmetric shifts for the different structures of the complexes are listed in Table 6.

The mononuclear bidentate (Figure 6D) and monodentate (Figure 6E) structures both predicted a downward shift for the $COO^-$ symmetric stretch to 1322 and 1342 $cm^{-1}$, respectively. Tejedor-Tejedor et al. attributed the $COO^-$ symmetric stretch to a peak at 1355 $cm^{-1}$,[31] which was good agreement with the

**TABLE 5: Experimental Peak Positions and Peak Assignmentsfor Phthalic Acid and $AlCl_3$[a]**

| solution Phth/$Al^{3+}$ | | adsorbed Phth/$Al_2O_3$ | | | phthalate | |
|---|---|---|---|---|---|---|
| pH 2.5 | pH 3.8 | pH 2.5 | pH 5 | pH 7 | pH 5 | peak assignments |
| 1695 | 1694 | 1692 | | | 1688 | C═O |
| 1602 | 1600 | 1604 | 1602 | 1604 | 1605 | C−C ring vib |
| 1582 | | | | 1583 | 1581 | $COO^-$ asym |
| | | | | | 1540 | C−C ring vib |
| 1487 | 1496 | 1489 | 1489 | 1489 | 1493 | C−C ring vib |
| 1478 | | | | | 1475 | C−C ring vib |
| 1449 | 1457 | 1446 | 1444 | | | C−C ring vib |
| 1405 | 1426 | 1405 | 1414 | 1403 | | $COO^-$ symmetric |
| 1378 | 1383 | | | | | $COO^-$ symmetric |
| | 1353 | | | | 1375 | $COO^-$ symmetric |
| | | | | 1364 | 1362 | $COO^-$ symmetric |
| | | | 1341 | | | $COO^-$ symmetric |
| 1296 | 1297 | 1298 | 1300 | 1310 | 1293 | C−C ring vib |
| 1270 | 1267 | 1263 | | | 1274 | C−OH |
| | | | | 1244 | | |
| 1170 | | | | 1174 | | C−H ip |
| | 1159 | 1157 | 1154 | | 1158 | C−H ip |
| 1146 | | | | | | C−H ip |
| 1045 | 1045 | 1043 | 1036 | 1063 | 1050 | C−H ip |

[a] Experimental peak positions for phthalic acid and $AlCl_3$ in solution at $10^{-2}$ M at the two pH values studied are shown in the first two columns. The salicylic and $AlCl_3$ were mixed in a one-to-one ratio. $Al^{3+}$ is not soluble above pH 4, thus the highest pH was 3.8 for the solutions. The next three columns show the experimental peaks for phthalic acid absorbed to $Al_2O_3$ at various pH values. The assignments in the last column are based on the theoretical predictions and previous assignments, which are discussed in the text.

**TABLE 6: Peak Positions for $COO^-$ Symmetric Stretches As Predicted by the Theoretical Frequency Calculations of the Optimized Structures Shown in Figure 6[a]**

| | Figure 6A | | Figure 6B | | Figure 6C | | Figure 6D | | Figure 6E | | Figure 6F | |
|---|---|---|---|---|---|---|---|---|---|---|---|---|
| | sym | asy | sym | asy | sym | asy | sym | asy | sym | asy | sym | asy |
| $COO^-$ peak positions | 1411 | 1543 | 1404 | 1533 | 1338 | 1648<br>1660 | 1322 | 1621<br>1642 | 1342 | 1529 | 1380 | 1534 |

[a] Two structures predicted two $COO^-$ asymmetric stretches.

**TABLE 7: Linear Fit Parameters from the Correlations of Experimental Data vs Theoretical Data for the Solutions of Phthalic Acid and Aluminum at $10^{-2}$ M and Salicylic Adsorbed to $Al_2O_3$[a]**

| | | monodentate | | | bidentate mononuclear | | | bridging bidenate (6ab) | | | bridging bidentate (6c) | | |
|---|---|---|---|---|---|---|---|---|---|---|---|---|---|
| sample | pH | slope | SD | $R^2$ | slope | SD | $R^2$ | slope | SD | $R^2$ | slope | SD | $R^2$ |
| Phth-$AlCl_3$ | 2.5 | 1.03 | 18.62 | 0.99 | 1.00 | 30.73 | 0.98 | 0.94 | 25.12 | 0.98 | 1.00 | 31.62 | 0.98 |
| | 3.8 | 1.01 | 21.01 | 0.99 | 0.99 | 31.88 | 0.98 | 0.95 | 22.91 | 0.99 | 0.96 | 20.83 | 0.99 |
| Phth-$Al_2O_3$ | 2.5 | 1.04 | 14.00 | 1.00 | 1.02 | 30.23 | 0.98 | 0.95 | 15.29 | 1.00 | 0.95 | 23.88 | 0.99 |
| | 4.8 | 1.04 | 13.54 | 1.00 | 1.06 | 29.07 | 0.98 | 0.98 | 11.13 | 1.00 | 1.08 | 24.57 | 0.99 |
| | 7* | 1.01 | 20.18 | 0.99 | 1.02 | 24.03 | 0.99 | 1.02 | 13.67 | 1.00 | 1.02 | 21.41 | 0.99 |

[a] The figures for the optimized structures are shown in Figure 6. The correct deprotonated structure was matched up for the correct pH (i.e., at pH 2.5 the monodentate structure is not deprotonated, at pH 3.8 it was). The type of bridging taking place is denoted by the figure listed after the name.

theoretical results. The deprotonated monodentate structure (Figure 6F) predicted two $COO^-$ symmetric stretches at 1380 and 1330 $cm^{-1}$. The peak at 1380 $cm^{-1}$ was attributed to the carboxylate group that was bonded to $Al^{3+}$, whereas the other was the deprotonated carboxylate group. The $COO^-$ asymmetric stretch position for the protonated and deprotonated monodentate structures (Figure 6E,F) were in good agreement with previous experimental results for phthalic and $Fe^{3+}$.[31] For the mononuclear monodentate structure (Figure 6D) there were two $COO^-$ asymmetric stretches calculated at 1621 and 1642 $cm^{-1}$ (Table 6), which was not in agreement with previous results.[22,31]

The structures in A and B of Figure 6 represent the bridging bidentate structures through one carboxylate group. For Figure 6A, the $COO^-$ symmetric stretch was calculated at 1411 $cm^{-1}$, and the $COO^-$ asymmetric was calculated at 1543 $cm^{-1}$. Figure 6B predicted $COO^-$ symmetric stretches at 1404 and 1357 $cm^{-1}$. The peak at 1404 $cm^{-1}$ was attributed to the carboxylate group that was complexed to $Al^{3+}$, and the 1357-$cm^{-1}$ peak was the uncomplexed group. For Figure 6B, there was an upward shift and a downward shift; this was significant for solutions above pH 5.4. If both peaks were observed, then it would be difficult to determine if more than one complex was present.

The last structure was that in Figure 6C, which was a bridging bidentate structure where one oxygen atom from each carboxylate group was bonded to an $Al^{3+}$. The calculated frequency of the $COO^-$ symmetric stretch was shifted down to 1338 $cm^{-1}$ and only one stretch was calculated. There were two asymmetric stretches predicted for this structure. Dobson et al. had predicted that this structure was representative of the phthalate$-Al_2O_3$ complex, with the $COO^-$ symmetric stretch observed at 1390 $cm^{-1}$.[22] There was no peak calculated in the 1370−1410 $cm^{-1}$ region for the structure in Figure 6E.

The theoretical calculations for the carboxylate symmetric stretch shifts agreed with the $\Delta\nu$ prediction method. With this good agreement, the correlation between the theoretical predictions and the experimental data was expected to be better. No single correlation could be considered as having the best fit for the solution data at pH 2.5 (Table 7). The problem has to do with multiple species for the metal−carboxylate complex being formed. Peaks for the symmetric stretch were observed at 1405 and 1378 $cm^{-1}$ for the solution at pH 2.5. The 1405-$cm^{-1}$ peak signifies that a bridging bidentate structure may be present as it was close to the calculated position for Figure 6A of 1411 $cm^{-1}$ (Table 6). The peak at 1378 $cm^{-1}$, assuming phthalic acid was in the form $HPhth^{-1}$ thus ruling out the structures in C and D of Figure 6, does not match with any calculated value.

This leaves two possibilities: (1) that the calculations are inaccurate even though they match reasonably well with previous results for $COO^-$ symmetric stretch positions or (2) uncomplexed phthalic acid was present. The peak at 1378 $cm^{-1}$ was a problem in all correlations, thus causing errors. The $COO^-$ symmetric peak was observed at 1375 $cm^{-1}$ and phthalic acid does not complex strongly at pH 2.5,[33] thus we suggest that the peak was due to uncomplexed phthalic acid. The bridging bidentate structure was formed for the $HPhth^{-1}/Al^{3+}$ complex at pH 2.5, with excess phthalic acid in solution. This conclusion is consistent with the weaker association constants measured for $Al^{3+}$−phthalate compared to $Al^{3+}$−salicylate.[34]

There were three peaks at 1426, 1383, and 1353 $cm^{-1}$ identified for the symmetric stretch for the solution of $HPhth^-/Al^{3+}$ at pH 3.8. The 1426 $cm^{-1}$ was shifted up from previous reports[17] and from the calculated positions for the bidentate structures (Table 6). The possibility that the peak was due to C−C vibrations has not been ruled out, but the lowest C−C ring vibration observed in solution was ∼1450 $cm^{-1}$ for solutions at pH 2.5 and pH 7.[19,30] At pH 2.5 the peak at 1383 $cm^{-1}$ was attributed to uncomplexed phthalic acid, whereas the peak at 1353 $cm^{-1}$ was attributed to the monodentate structure for two reasons. The first was that the correlation between experimental and theoretical data was better than that of the mononuclear monodentate structure (Table 7; A and B in Figure 8). The second reason was due to the position of the $COO^-$ symmetric stretch being in better agreement with the monodentate than with the mononuclear monodentate structure calculated position (Table 6).

For the adsorbed sample at pH 2.5, there was only one peak observed for the symmetric stretch at 1405 $cm^{-1}$. This position was in good agreement with the calculated frequency for the complex in Figure 6A, but overall the correlation between model and experiment was not good (Table 7). There were no outliers, but the slope was only 0.95, which was not as good agreement as we have previously obtained. However, this correlation had an excellent standard deviation (15.29) and an $R^2 = 1$ (Table 7). The monodentate complex had a slightly better standard

**TABLE 8: The Predicted Structures for the UVRR Method and Theoretical Method for the Different Samples Are Summarized**[a]

| sample | pH | experimental | theoretical |
|---|---|---|---|
| HPhth/$AlCl_3$ | 2.5 | bridging bidentate | bridging bidentate |
| | 3.8 | bridging bidentate monodentate | bridging bidentate (doubtful) monodentate |
| HPhth/$Al_2O_3$ | 2.5 | bridging bidentate | bridging bidentate |
| | 4.8 | bridging bidentate/ monodentate | bridging bidentate/ monodentate |
| | 7 | bridging bidentate | bridging bidentate (1e) |

[a] The structures for the UVRR method were based on previous reports that reported shifting of vibrational modes for different complexes. The theoretical method was fit to the experimental data from UVRR.

deviation (14.00) and slope (1.04), but the position of the symmetric stretch does not correlate with the monodentate structure. The 1405-$cm^{-1}$ peak was attributed to a C−C ring stretch at 1430 $cm^{-1}$ in the monodentate correlation. The bridging bidentate structure was the predicted structure for this sample because of the position of the $COO^-$ symmetric stretch.

For the adsorbed sample at pH 4.8, there were two peaks attributed to the $COO^-$ symmetric stretch at 1414 and 1341 $cm^{-1}$. The peak at 1414 $cm^{-1}$ corresponds to Figure 6a (Table 7), which also had the best fit with a slope of 0.98, standard deviation of 11.13, and an $R^2$ of 1.00 (Table 7). The experimental peak at 1341 $cm^{-1}$ was correlated with a calculated peak at 1311 $cm^{-1}$ attributed to a ring vibration coupled to a C−O−H stretch. The experimental peak at 1341 $cm^{-1}$ correlates well with the monodentate structure predicted symmetric stretch at 1342 $cm^{-1}$. The correlation for the monodentate had a slope of 1.04, standard deviation of 13.54, and an $R^2$ of 1.00 (Table 7). The experimental peak at 1414 $cm^{-1}$ was fit to the 1430 $cm^{-1}$ calculated peak attributed to C−C ring vibration. The two structures that were present in this sample were the monodentate (Figure 4E) and the bridging bidentate (Figure 6A). These findings were in agreement with results from studies on phthalic acid and iron complexes.[31]

There were also two peaks observed for the $COO^-$ symmetric stretch on the adsorbed sample at pH 7. They were at 1403 and 1364 $cm^{-1}$, which correlated well with the calculated positions at 1404 and 1357 $cm^{-1}$ for the structures in B and E of Figure 6 (Table 6). This also gave the best fit with a slope of 1.02, standard deviation of 13.67, and an $R^2$ of 1.00 (Table 7). The monodentate structure had a better slope (1.01), but the standard deviation (20.18) was higher (Table 7). The other factor was that the calculated symmetric stretch for the monodentate structure was at 1342 $cm^{-1}$, thus the bridging bidentate structure matched the symmetric stretch better.

Table 8 summarizes the different structures that were found for the complex between phthalate and $Al^{3+}$. The mononuclear bidentate structure was not observed for any of the samples, which was not in agreement with Dobson et al.[22] Tejedor-Tejedor et al. suggested both bridging bidentate (Figure 6A) and monodentate (Figure 6E) structures for complexes of HPhth/Fe, thus our findings support the interpretations of Tejedor-Tejedor et al.[31] assuming phthalate $Al^{3+}$ and $Fe^{3+}$ complexation are similar. There was strong similarity between the spectra of solutions and those of the surface species. The appearance of the monodentate structure between pH 4 and 5, but not at pH 2.5 or 7, was puzzling. For the salicylic and $Al^{3+}$, there was a trend, but a trend was not observed for phthalic acid. One possibility was that it was present at one or both of the other pH values, but was not observed. Phthalic acid absorbs UV most strongly at pH 4,[33] which may be the reason that it was observed at pH 3.8 and 4.8 and not the other pH values.

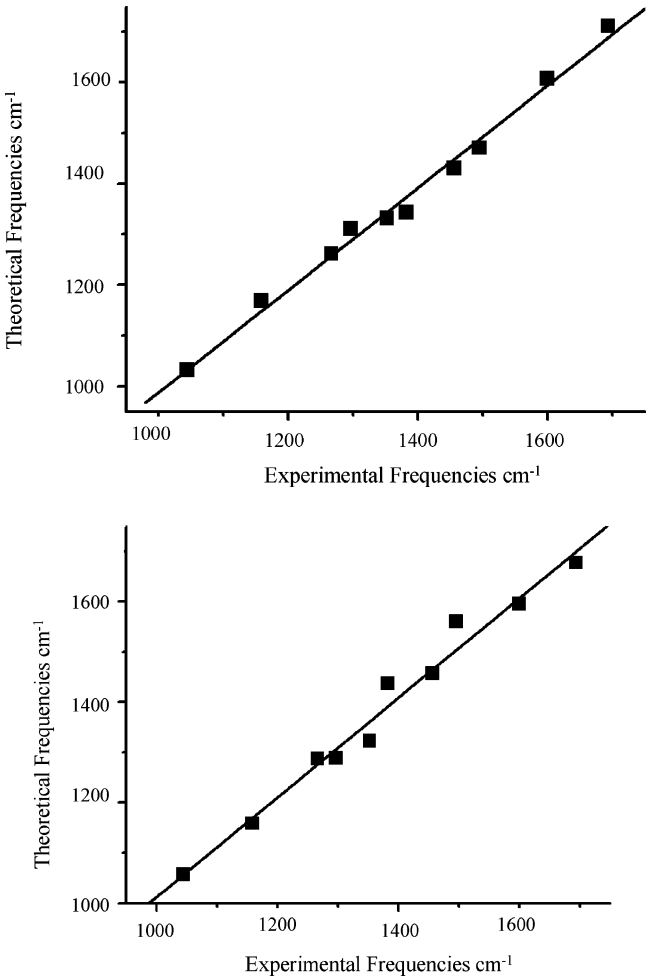


**Figure 8.** Linear correlations of the theoretical frequencies for the monodentate and mononuclear bidentate structures to the experimental UVRR frequencies of phthalic acid at pH 2.5. Table 7 contains the linear fit parameters.

**Comparison to Potentiometric Modeling Studies.** A number of studies have been published on Al−salicylate complex thermodynamics.[35−38] However, it is difficult to use these results to predict the speciation under the conditions of our experiments. First, the salicylate/$Al^{3+}$ ratios are generally greater than 1:1 in most potentiometric studies to prevent precipitation of $Al(OH)_3$ above a pH of ∼2.[38] Another problem is that the mononuclear bidentate species $AlL^+$ (where salicylate is doubly deprotonated) has been derived in the modeling of the potentiometric data.[38] Kummert and Stumm [25] recognized that this bidentate complex should not be the dominant species below a pH of 3.8 (6.6 for a surface complex). Thus, although association constants are available that would predict the amount of Al−salicylate complexation, it was difficult to extrapolate these values to the conditions of our experiment or apply them at all when the species may be incorrect. We do assume that for our salicylate/$Al^{3+}$ ratios of 1:1, the 1:1 complex will generally be dominant over any $Al(sal)_2$ or $Al(sal)_3$ species. The fact that our model calculations agree with the observed frequencies and explain the observed bands is justification for this assumption.

Nordstrom and May [36] stated that Raman spectroscopy was not suited for the study of these complexes because it does not measure the thermodynamic properties. While this is true, Raman spectroscopy does allow one to observe the frequencies of the carboxylic acids and the changes they undergo with the

addition of $Al^{3+}$ and change in pH range. Thus, one can observe the bonding properties to determine whether the assumption of a bidentate complex for the potentiometric experiments was correct. Once the correct structure or structures have been identified, then one can use the speciation to fit the potentiometric measurements rather than using the assumed speciation from the potentiometric models to interpret spectra.

As an example of the possible discrepancies between potentiometric modeling and spectroscopic observations, we have calculated the association of $Al^{3+}$ and salicylate for a typical solution in this study. Experimental equilibrium constants, *K*, values based on the reaction

$$Al^{3+} + L \leftrightarrow AlL$$

vary from 12.9 to 14.5[36] where $n = 1$. An average of 13.5 was used here. The equation for *K* is

$$K = [AlL]/([AlL][L])$$

with units of inverse concentration. If we were to substitute our concentrations ($10^{-2}$ M) into this equation, then we would obtain a concentration of for $AlL_{n-1}$ of $1.35 \times 10^{-3}$ M, which would indicate approximately 13% of the salicylate was complexed. If this were the case, then most of the salicylic acid would be uncomplexed, which would be visible in the Raman or IR spectra by comparison to the spectra without $Al^{3+}$ present. The fact that we did not observe uncomplexed salicylic in these spectra indicates that these equilibrium complexes may underestimate the amount of complexation in this case. There could be uncomplexed salicylic in our solutions, but the concentration must be small compared to that of the complexed ligand.

The root of the discrepancy is that the potentiometric data are fit to obtain association constants, $\beta_{p,q,r}$, of model reactions such as[38]

$$pH^+ + qAl^{3+} + r(H_2L) \leftrightarrow H_pAl_q(H_2L)_r^{p+3q}$$

The titration data are then fit with a variety of *p*, *q*, and *r* parameters, and the set that gives the smallest error is selected assuming that only one type of complex forms. In addition, it is assumed that the $pK_a$ of the ligand and the hydrolysis constant of the metal do not change in the mixed system. There are complicating factors that could make the model reactions incorrect (e.g., hydrolysis and/or oligomerization of the $Al^{3+}$,[39] changing $pK_a$ values with complexation[25]). Although the model reactions in many of these studies may be correct under certain concentrations and pH ranges, they must be independently verified before the derived association or equilibrium constants can be considered correct. Verification of the speciation based on spectroscopy and modeling of the vibrational frequencies is the main goal of this paper. These species can then be used to model the potentiometric data and derive new association constants.

## Summary

This work has demonstrated that Al−organic acid complexes in solutions and on the $Al_2O_3$ surface are related. The same acid/metal complexes were suggested in two different environments. As long as the acid was in the same form (i.e. neutral or anion or bianion) the complexes were the same. This indicates that it is the pH of the solution and not the environment that controls complexation of salicylic and phthalic acids with $Al^{3+}$. It is uncertain if this would hold true for other aromatic carboxylic acids and further experiments should be performed.

There were excellent correlations between the theoretical predictions and experimental evidence for the types of complexes that we assigned to the experimental spectra. In a few cases, there was more than one model with a correlation that was excellent. This came about because there were a limited number of vibrational frequency differences between the two model complexes. Using multiple experimental techniques with the theoretical work has been shown to be valuable in clearing up any confusion. With salicylic acid, there were two structures with close agreement to the experimental results for UVRR, but the NMR results agreed with our suggested structure from the UVRR. Having results from other techniques would be beneficial for phthalic acid where we observed multiple structures for the anion species.

**Acknowledgment.** This research was funded by NSF grant CHE-0089156 (Molecular level analysis of macromolecule-surface interactions in bacterial adhesion) and Stony Brook-BNL collaboration to establish a Center for Environmental Molecular Sciences (CEMS). The researchers would also like to thank John Badding at Pennsylvania State University for the use of the UVRR spectrometer. We would also like to thank Bryan Jackson for technical help. Computation was supported in part by the Materials Simulation Center, a Penn-State MRSEC and MRI facility.

## References and Notes

(1) Alexander, M. *Environ. Sci. Technol.* **1995**, *29*, 2713.
(2) Leenheer, J. A.; Brown, P. A.; MacCarthy, P.; Cabaniss, S. E. *Environ. Sci. Technol.* **1998**, *32*, 2410.
(3) Elkins, K. M.; Nelson, D. J. *Coord. Chem. Rev.* **2002**, *228*, 205.
(4) Tan, K. H. *Humic Matter in Soil and the Environment*; Marcel Dekker: New York, 2003.
(5) Hayes, M. H. B.; MacCarthy, P.; Malcolm, R. L.; Swift, R. S. *Humis Substances II, In Search of Structure*; John Wiley & Sons: New York, 1989.
(6) Biber, M. V.; Stumm, W. *Environ. Sci. Technol.* **1994**, *28*, 763.
(7) Thomas, F.; Maslon, A.; Bottero, J. Y.; Rouiller, J.; Montigny, F.; Genevrier, F. *Environ. Sci. Technol.* **1993**, *27*, 2511.
(8) Yost, E. C.; Tejedor-Tejedor, I.; Anderson, M. A. *Environ. Sci. Technol.* **1990**, *24*, 822.
(9) Kubicki, J. D.; Itoh, M. J.; Schroeter, L. M.; Aptiz, S. E. *Environ. Sci. Technol.* **1997**, *31*, 1151.
(10) Stumm, W. *Chemistry of the solid−water interface: Processes at the mineral−water and particle−water interface in natural systems*; Wiley: New York, 1992.
(11) Munro, C. H.; Pajcini, V.; Asher, S. A. *Appl. Spectrosc.* **1997**, *51*, 1722.
(12) Frisch, M. J.; Trucks, G. W.; B.Schlegel, H.; Scuseria, G. E.; Robb, M. A.; Cheeseman, J. R.; Zakrzewski, V. G.; Montgomery, J. A., Jr.; Stratmann, R. E.; Burant, J. C.; Dapprich, S.; Millam, J. M.; Daniels, A. D.; Kudin, K. N.; Strain, M. C.; Farkas, O.; Tomasi, J.; Barone, V.; Cossi, M.; Cammi, R.; Mennucci, B.; Pomelli, C.; Adamo, C.; Clifford, S.; Ochterski, J.; Petersson, G. A.; Ayala, P. Y.; Cui, Q.; Morokuma, K.; Salvador, P.; Dannenberg, J. J.; Malick, D. K.; Rabuck, A. D.; Raghavachari, K.; Foresman, J. B.; Cioslowski, J.; Ortiz, J. V.; Baboul, A. G.; Stefanov, B. B.; Liu, G.; Liashenko, A.; Piskorz, P.; Komaromi, I.; Gomperts, R.; Martin, R. L.; Fox, D. J.; Keith, T.; Al-Laham, M. A.; Peng, C. Y.; Nanayakkara, A.; Challacombe, M.; Gill, P. M. W.; Johnson, B.; Chen, W.; Wong, M. W.; Andres, J. L.; Gonzalez, C.; Head-Gordon, M.; Replogle, E. S.; Pople, J. A. *Gaussian 98*, Revision A.10; Gaussian, Inc.: Pittsburgh, PA, 2001.
(13) Lee, C.; Yang, W.; Parr, R. G. *Phys. Rev. B* **1988**, *37*, 785.
(14) Becke, A. D. *J. Chem. Phys.* **1993**, *98*, 5648.
(15) Krishnan, R.; Binkley, J. S.; Seeger, R.; Pople, J. A. *J. Chem. Phys.* **1980**, *72*, 650.
(16) McLean, A. D.; Chandler, G. S. *J. Chem. Phys.* **1980**, *72*, 5639.
(17) Trout, C. C.; Kubicki, J. D. Submitted for publicaiton.
(18) Wong, M. W.; Wiberg, K. B. *J. Chem. Phys.* **1991**, *95*, 8991.
(19) Joo, S. W.; Han, S. W.; Han, H. S.; Kim, K. *J. Raman Spectrosc.* **2000**, *31*, 145.
(20) Humbert, B.; Alnot, M.; Quiles, F. *Spectrochim. Acta A* **1998**, *54*, 465.
(21) Tejedor-Tejedor, I. M.; Yost, E. C.; Anderson, M. A. *Langmuir* **1990**, *6*, 979.

(22) Dobson, K.; McQuillan, A. J. *Spectrochim. Acta A* **2000**, *56*, 557.
(23) Phambu, N. *Appl. Spectrosc.* **2002**, *56*, 756.
(24) Kubicki, J. D.; Blake, G. A.; Aptiz, S. E. *Geochim. Cosmochim. Ac.* **1996**, *60*, 4897.
(25) Kummert, R.; Stumm, W. *J. Colloid Interface Sci.* **1980**, *75*, 373.
(26) Clausén, M.; Öhman, L.-O.; Kubicki, J. D.; Persson, P. *J. Chem. Soc., Dalton* **2002**, *12*, 2559.
(27) Foresman, J. B.; Frisch, A. *Exploring Chemistry with Electronic Structure Methods*; Gaussian, INC.: Pittsburgh, PA, 1993.
(28) Kubicki, J. D.; Sykes, D.; Aptiz, S. E. *J. Phys. Chem. A* **1999**, *103*, 903.
(29) Colombo, L.; Volovsek, V.; LePostollec, M. *J. Raman Spectrosc.* **1984**, *15*, 252.
(30) Loring, J. S.; Karlsson, M.; Fawcett, W. R.; Casey, W. H. *Spectrochim. Acta A* **2001**, *57*, 1635.
(31) Tejedor-Tejedor, M. I.; Yost, E. C.; Anderson, M. A. *Langmuir* **1992**, *8*, 525.
(32) Nakamoto, K. *Infrared and Raman Spectra of Inorganic and Coordination Compounds*; Wiley: New York, 1986.
(33) Lovgren, L. *Geochim. Cosmochim. Ac.* **1991**, *55*, 3639.
(34) Hue, N. V.; Craddock, G. R.; Adams, F. *Soil Sci. Soc. Am. J.* **1986**.
(35) Secco, F.; Venturini, M. *Inorg. Chem.* **1975**, *14*, 1978.
(36) Nordstrom, D. K.; May, H. M. Aqeous equilbrium data for mononuclear aluminum species. In *The Environmental Chemistry of Aluminum*, 2nd ed.; Sposito, G., Ed.; CRC Press: New York, 1996; p 39.
(37) Martell, A. E.; Smith, R. M. *Critical Stability Constants*; Plenum Press: New York, 1977.
(38) Öhman, L. O.; Sjöberg, S. *Acta Chem. Scand. A* **1983**, *37*, 875.
(39) Tossell, J. A. *J. Magn. Reson.* **1998**, *135*, 203.